# PROBLEMS AND INFORMATICS-AIDED SOLUTIONS IN RESEARCH OF NEURODEGENERATION WITH AN EMPHASIS ON QUANTITATIVE MORPHOLOGY

Ph.D. Thesis by

**Tamás Ferenc Polgár**

Supervised by:

**Bernát Nógrádi**, M.D., Ph.D.

**Roland Patai**, Ph.D.

Laboratory of Neuronal Plasticity, Molecular Neurobiology Research Unit,
Institute of Biophysics, HUN-REN Biological Research Centre, Szeged, Hungary

Doctoral School of Experimental and Preventive Medicine, University of Szeged, Hungary

Neuroscience Research Group, Department of Neurology, University of Szeged, Hungary

**Szeged**

**2025**

## Introduction

The human nervous system contains hundreds of billions of neurons and glial cells, but their number and morphology change in almost any neuronal disease and even in healthy ageing. Therefore, to characterize cell number and morphological changes is essential in understanding pathological processes, which is the first step in a lengthy course of investigations to develop treatments to slow disease progression and ultimately cure the patients.

The type of neurons affected depends on the disease itself – for instance, in the case of amyotrophic lateral sclerosis (ALS), which is in the focus of our research, the motor neurons in the motor cortex and in the spinal cord are impacted by the degenerative processes. Thus, before counting or characterizing the morphology of cells, first, a sampling paradigm must be established, specifying tissue type, anatomical regions of interest, sub-regions, etc. (Figure 1.) Then, finding – or developing - a correct method to count cells, especially using conventional microscopy of thin sections is a delicate task.

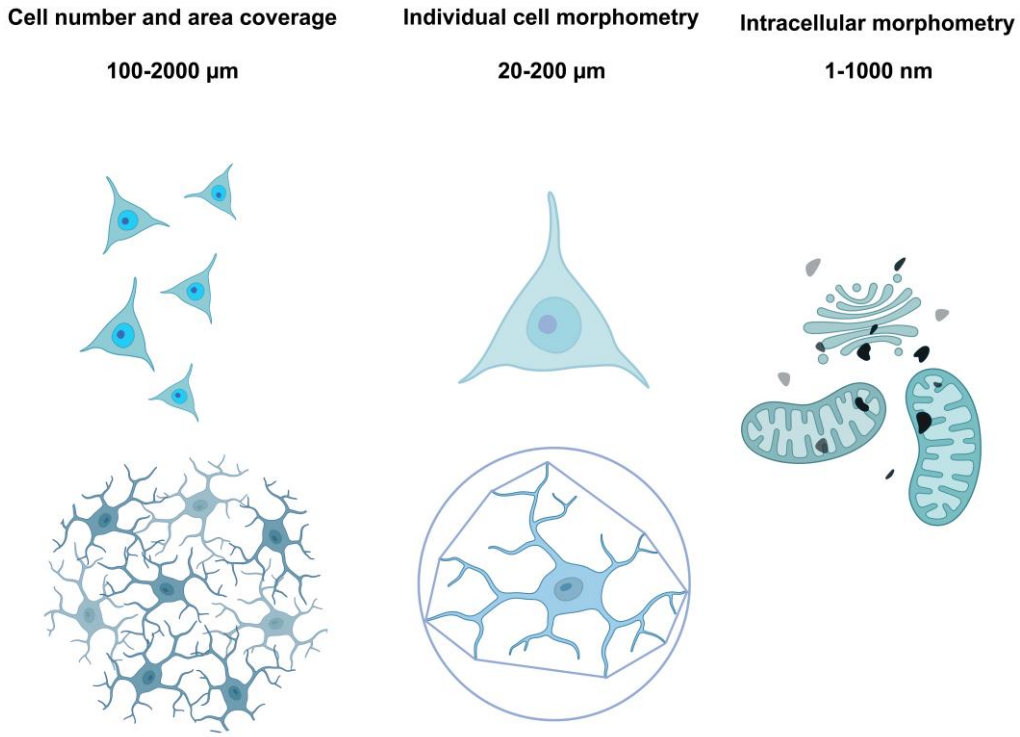


***Figure 1.*** *Scheme of hierarchic sampling for morphological characterization of neural and microglial cells at light (anatomical region, cell populations and individual cells) and electron microscopic (intracellular components) level.*

The goal of experimental neurology research is to better understand the pathomechanisms underlying human neurodegenerative diseases, to slow down or eventually halt disease

progression. Since human brain samples, due to ethical considerations, are only available for direct examination in exceptional cases, experimental models mimicking certain aspects of the investigated disease are utilized. Since the spinal cord and brain samples of these animals could be similarly characterized, the observations in these regions of the central nervous system enabled the extrapolations to the human central nervous system. In the first part of the thesis, the relationship of the loss of spinal motor neurons and the change of their calcium homeostasis, which plays a central role in degenerative processes, is examined in an animal model of ALS.

Immunofluorescence (IF) microscopy has the advantage of multiple staining and simultaneous visualization of different cells and cellular compartments. However, IF with quantitative evaluation is rather challenging due to photobleaching, which is a well-known phenomenon that occurs when fluorophores lose their ability to emit fluorescence upon prolonged exposure to excitation light. This weakening in fluorescence may particularly affect the morphological characterization of objects with fine process arborization, for example, microglia and astrocytes, altering the obtainable data using image analysis. The magnitude of the effect of photobleaching on quantitative morphometric parameters of fluorescently labelled cells, however, is not known in detail. In the next part of the thesis, the results of our experiments characterizing this phenomenon are presented.

The utility of animal models of neurodegenerative diseases is not limited to the availability of the entire nervous system for different types of examinations but also provides a shorter duration for the development of the disease and the possibility of introducing and testing potential medical treatments. In human neurodegenerative diseases, however, any potential treatment is delayed by the relatively long diagnostic time. Since ALS shows heterogeneous progression and symptoms, there is no single test for the disease, thus, the diagnosis is based on a combination of inclusion and exclusion clinical criteria. Consequently, the disease has an exceptionally long diagnostic time (from symptom onset to confirmed diagnosis, the time range is from half to one and a half years).

The question asked by Mitchell et al. in the title of their paper published in 2010, “Can we do better?” was also investigated in the thesis by showing a simple, AI-generated example of automatizing repetitive image analysis and evaluating the potential supporting role of artificial intelligence in setting up or facilitating diagnosis of neurodegenerative diseases.

**Aims**

Characterization of the motoneuronal calcium level and loss of motor neurons in a model of ALS using optimized dissector methods

Characterization of the effect of photobleaching on the morphometric analysis of fluorescently labeled cells in the central nervous system

Characterization of the potential supportive role of artificial intelligence in image analysis and the diagnosis of neurological diseases

## Results

### Effect of passive transfer of ALS sera on survival of motor neurons and intracellular calcium

#### *Loss of lumbar motor neurons in mice after injection of ALS sera*

Results did not show any alteration in the number of motor neurons (MNs) in the lumbar spinal cord after passive transfer from healthy individuals compared to the untreated animals (Figure 2A, B), however, passive transfer of ALS sera resulted in a prominent loss of MNs (Figure 2C).

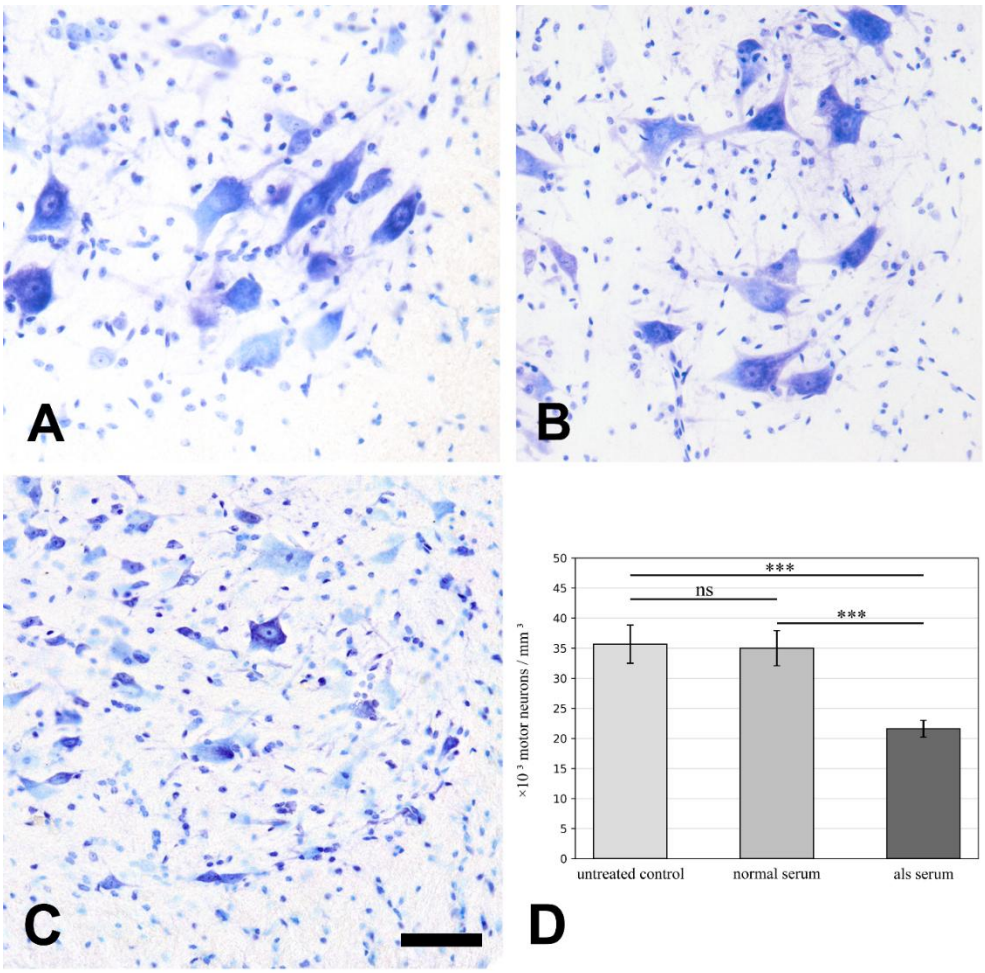


***Figure 2.*** *Large cells (>30 µm of characteristic profile size) identified as MNs are detectable in high numbers in untreated mice (n = 3) (A) or after injection with sera from healthy individuals (n = 3) (B). A reduction in the number of MNs was observed after treatment with serum from ALS patients (n = 14) (C). Scale bar: 100 µm.*

#### *Changes in the calcium content of motor neurons after Injection of ALS sera*

Significant MN loss can be observed in the ventrolateral MN pool in the ALS model compared to the controls; however, subtler markers of degeneration can also be noted if we investigate

subcellular elements of the still-detectable cells. With electron microscopy, no ultrastructural alteration could be seen in MNs of untreated mice or after treatment with serum from healthy controls (Figure 3A, B). After inoculation with ALS sera, disorganized mitochondrial cristae, dilated endoplasmic reticulum and Golgi complex can be observed in the perikarya of MNs compared to controls. Increased cytoplasmic and mitochondrial calcium, visualized as a larger number of electron-dense deposits (EDDs), could be observed in MNs after treatment with sera from ALS patients (Figure 3C, Figure 4).

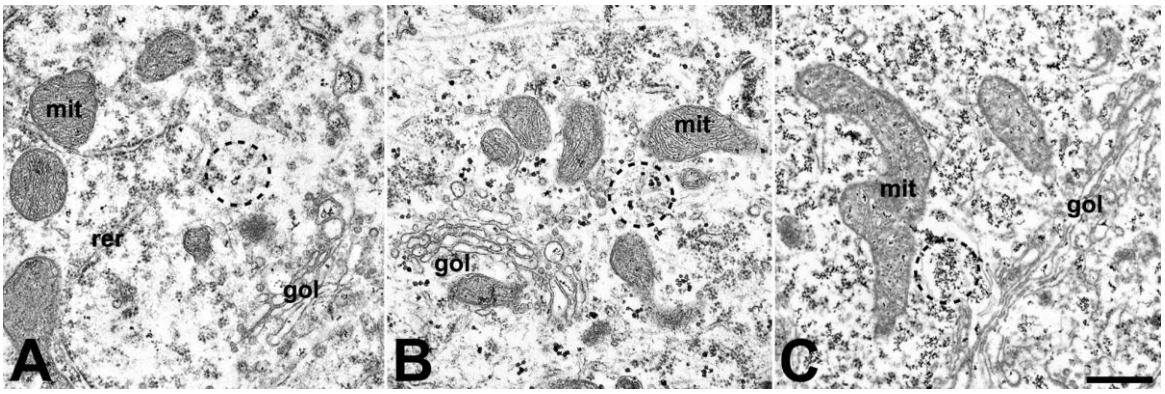


***Figure 3.*** *Ultrastructural alterations can be seen in the micrographs of motor neurons from mice treated with sera from amyotrophic lateral sclerosis (ALS) patients (C) compared to untreated (A) and the healthy serum-treated samples (B). Mit: mitochondrion; rer: rough endoplasmic reticulum; gol: Golgi complex; Scale bar: 500 nm.*

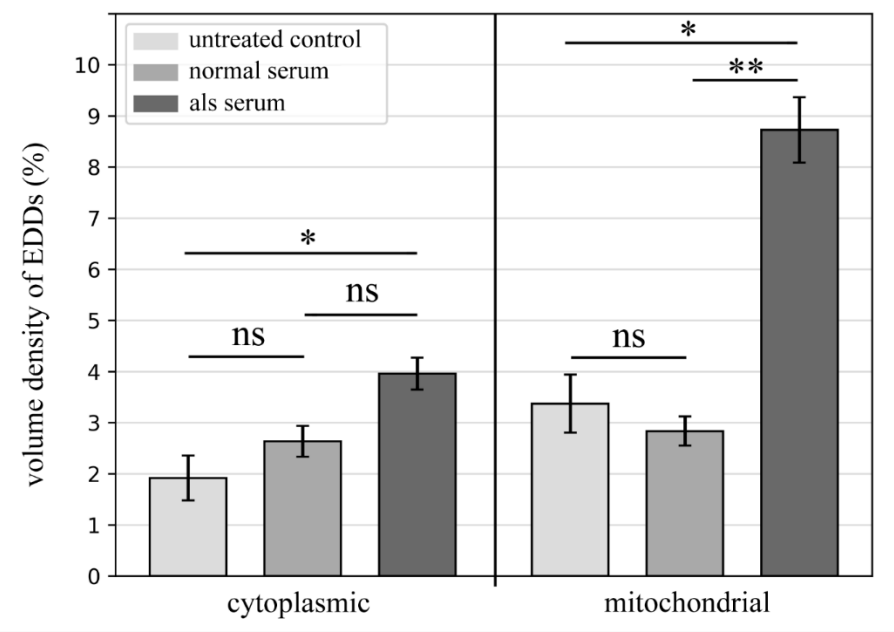


***Figure 4.*** *A significant elevation in electron-dense deposits can be observed in cytoplasmic and mitochondrial regions of the motor neurons (MNs) of the ALS sera-treated mice (n = 30)*

*compared to untreated mice (n = 3) or mice treated with serum from healthy individuals (n = 3).*

***Correlation of intracellular calcium increase and loss of motor neurons***

Correlation analysis revealed a strong negative correlation between the number of surviving MNs and intracellular calcium level increase in the spinal cord MNs (Figure 5). The data representing the control groups (untreated and control serum-treated groups) were separated from the ALS serum-treated patients' data. Furthermore, in the ALS serum-treated group, one subpopulation emerged; as cluster analysis separated the data representing the mice which received serum from ALS patients with a mutation in the chromosome 9 open reading frame 72 (C9ORF72) gene. This subpopulation of ALS serum-treated mice displayed more severe MN loss and highly increased intracellular calcium levels.

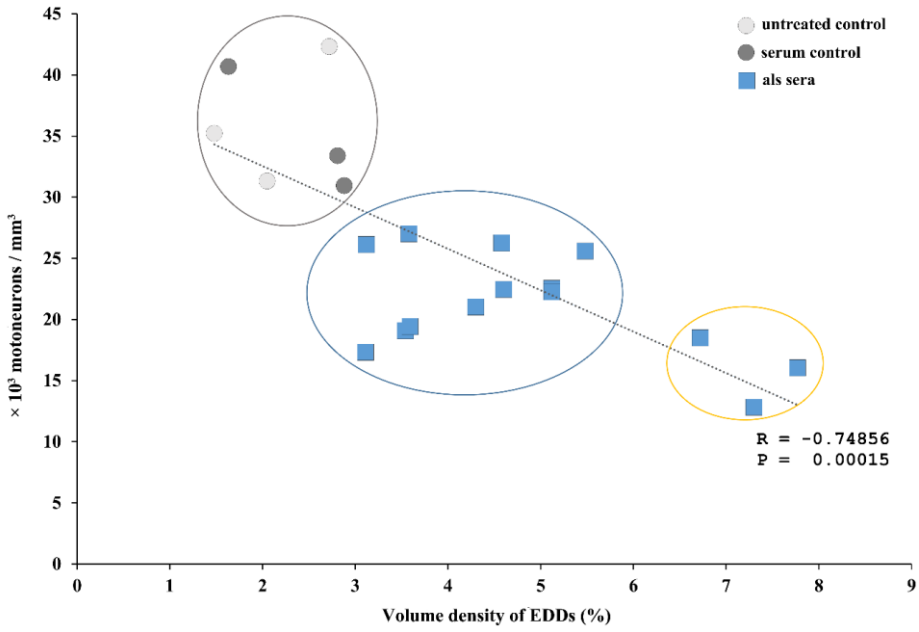


***Figure 5.*** *Each symbol (except for the untreated animals) represents a patient who served as a serum donor. The number of surviving spinal motor neurons negatively correlated with the increase in intracellular calcium levels. Three clusters could be identified: the control group (at the left side), the majority of the ALS patients (at the middle), and a subgroup of ALS patients with chromosome 9 open reading frame 72 hexanucleotide repeats (at the right side).*

**Effect of photobleaching on the morphometric analysis of fluorescently labeled cells**

***Effect on mean signal intensity***

In order to determine the adequate method for a larger-scale (individual cell morphology and cell populational measurements) morphological evaluation on neurons and microglia, first, mean signal intensity was measured in large field of view images after neuronal and microglial staining using A488 and A546 fluorophores (Figure 6).

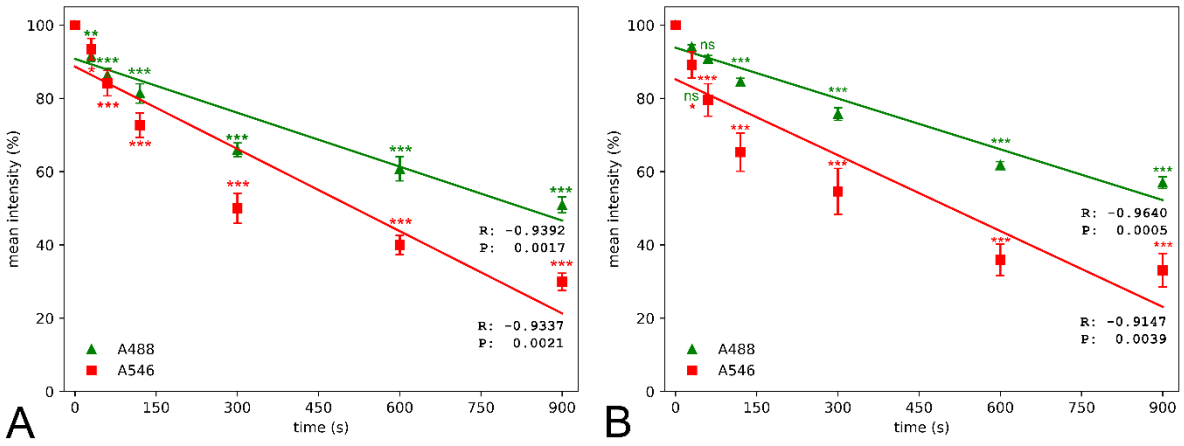


***Figure 6.*** *Quantitative determination of mean pixel intensity revealed that photobleaching led to a significant decrease of the fluorescent light as early as after 30-60 seconds compared to values at zero illumination time of microglial (A) (Iba1) and neuronal staining (B) (NeuN).*

***Effect on the number of detectable neurons***

Neurons in the spinal cord were counted in the same area with different illumination times, if their nuclei could still be identified (Figure 7). The number of detectable neuronal profiles was reduced by approximately 10% after 60 seconds of illumination of samples, regardless of the fluorophore. At the end of the experiment, A488 showed a 22% decrease in the number of detectable neurons, but more than half of the initial number of neuronal profiles became unidentifiable if samples were stained with A546.

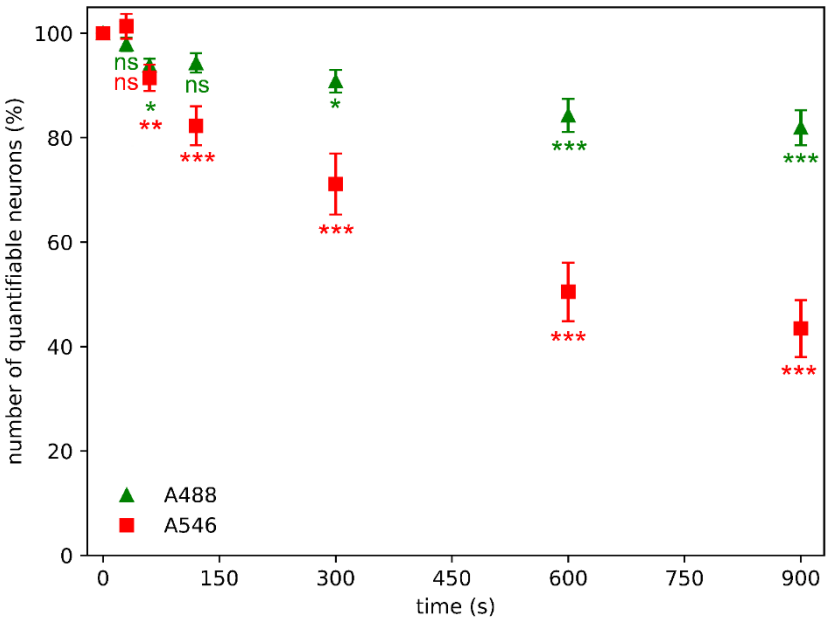


***Figure 7.*** *Photobleaching has a significant effect on quantifiable neuronal number (stained neurons with discernible nucleus) even after 60 seconds of illumination time using Alexa Fluor 546 (A546) (n = 15) and Alexa Fluor 488 Plus (A488) (n = 15) compared to the values measured at zero sec illumination time.*

***Effects on relative area coverage and area fraction of microglial cells***

The cell-to-background-relative microglial profile area coverage measurement maps the background density and standard deviation of the background to provide a cut-off value of the image of interest for segmentation. Same areas at different time points were acquired, and the relative differences between the actual image and the initial image were calculated (Figure 8).

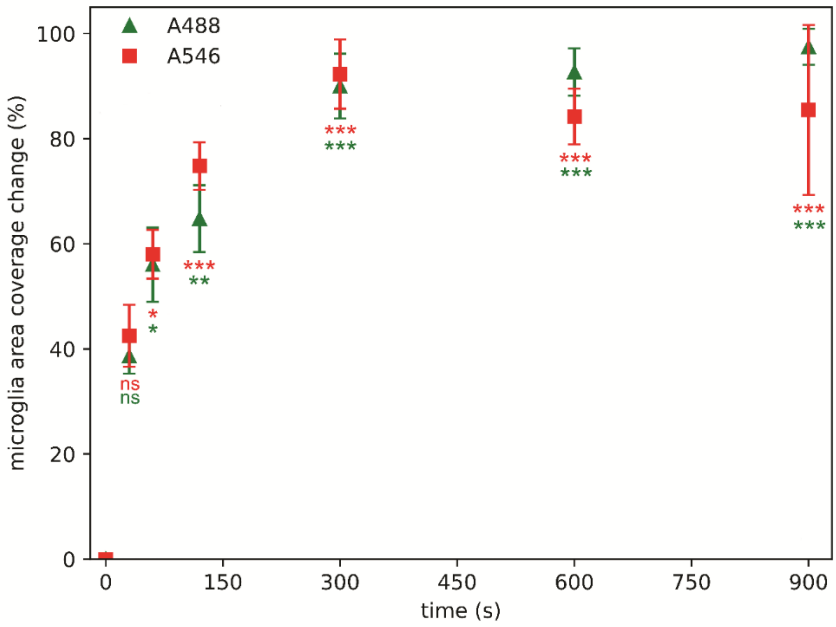


***Figure 8.*** *Photobleaching has a significant effect on microglial area coverage measurements even after 60 seconds of illumination time using Alexa Fluor 546 (A546) (n = 15) and Alexa Fluor 488 Plus (A488) (n = 15) compared to area coverage measured at zero time point.*

The ImageJ-based, ChatGPT-generated macro, performing image transformations, user-controlled thresholding with binarization and area fraction parameter-retrieval, was used to evaluate the images, in parallel to the Image Pro-Plus macro-based quantification. Notable changes first occurred after 30 (A488) and 120 (A546) seconds of illumination (Figure 9). The ChatGPT-generated ImageJ macro revealed similar changes as the manually-prepared Image Pro-Plus macro (Figure 8, Figure 9).

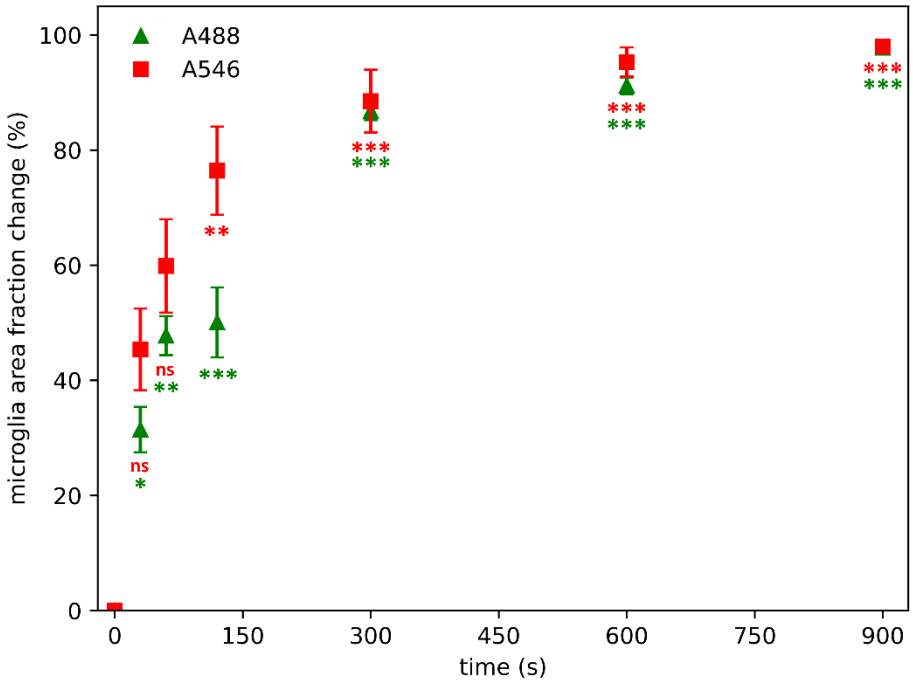


***Figure 9.*** *Quantification of microglial area coverage alterations with the ChatGPT-generated ImageJ macro. Photobleaching has a significant effect on microglial area fraction measurements even after 30 seconds of illumination time using Alexa Fluor 488 Plus (n = 15) compared to area fraction measured at zero time point.*

### *Effects on fractal parameters of microglia cell profiles*

Morphometric parameters were compared between individual cell profiles segmented from images taken at different time points (Figure 10). Based on the mean intensity changes and considering the time-consuming process of semi-manual segmentation, cell profiles were segmented at the 0-time point and at a determined endpoint of illumination time where the binarization process still could be done. This time was 120 seconds for A546 and 900 seconds for A488. Different parameters show different levels of resistance to photobleaching.

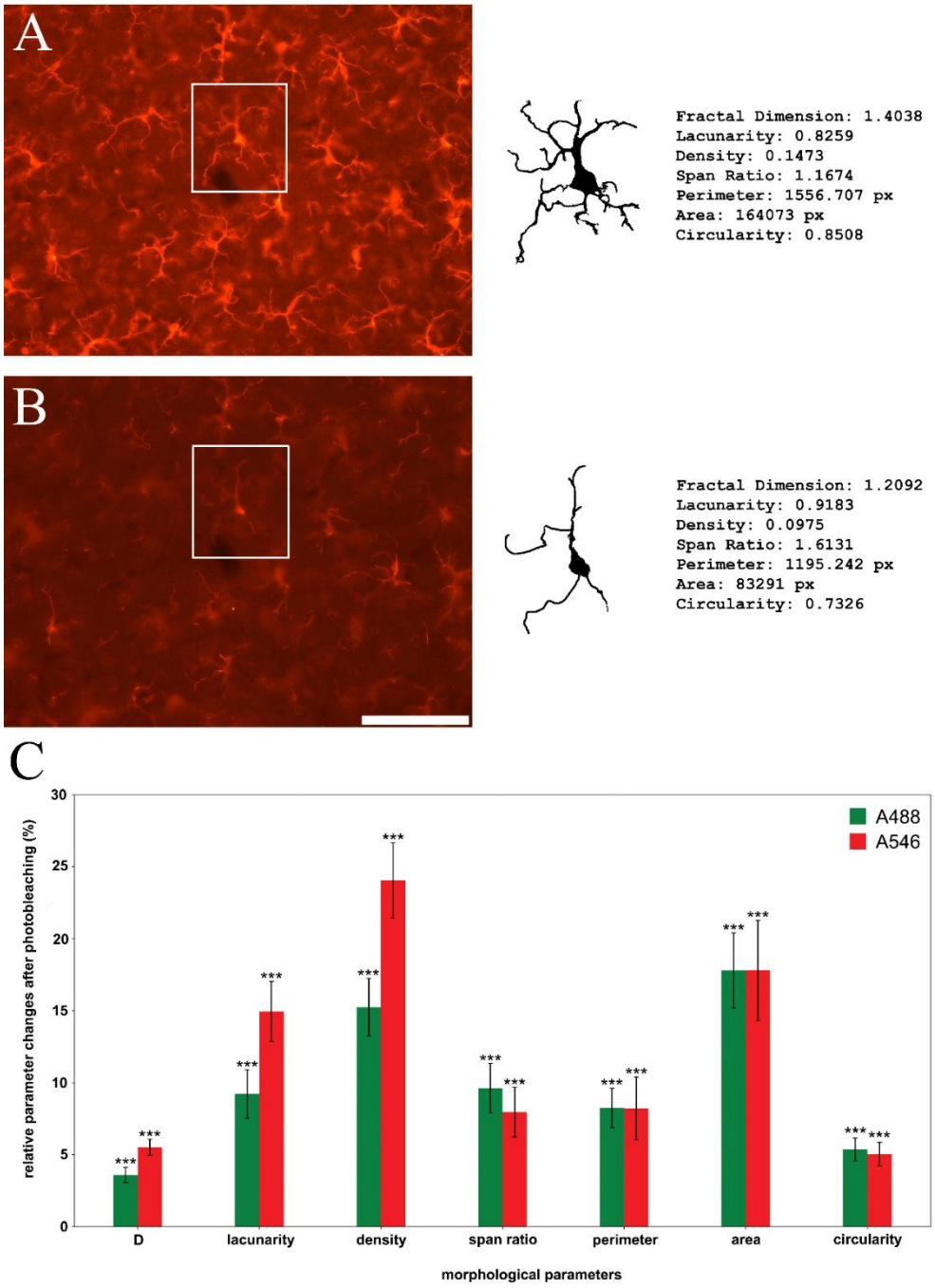


***Figure 10.*** *Photobleaching has a significant effect on morphological parameters of individual microglial cell profiles (A: initial image, B: faded image) using Alexa Fluor 546 (A546; red bars on panel C) (n = 30) and Alexa Fluor 488 Plus (A488; green bars on panel C) (n = 30). D: fractal dimension. Scale bar: 100 µm.*

***Combination of the DAB-Based and the Fluorescent-Based Immunohistochemistry***

For morphological quantification within identified anatomical structure, the DAB-based and the fluorescent based immunohistochemistry in a single section were combined (Figure 11). The fluorescently stained MNs are used to identify the border of the hypoglossal nucleus, which

border is then copied to the DAB-stained microglial stained image, and the microglial area coverage could be determined within this border. For illustration of the co-distribution, the two images are overlaid.

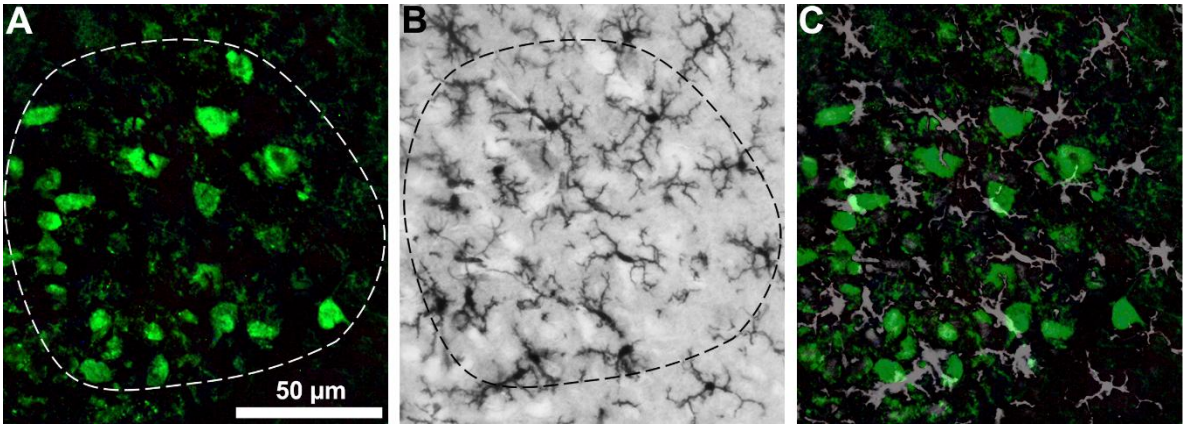


***Figure 11.*** *The fluorescently stained (ChAT-positive) motor neurons are used to identify the border of the hypoglossal nucleus (A), then the borderline is copied to the DAB-stained (Iba1-positive) microglial stained image (B), and the microglial area coverage could be determined within this border. For illustration of the co-distribution, the two images are overlaid (C). Scale bar: 50 µm.*

**Testing diagnostic potential of artificial intelligence in neurological diseases**

***Diagnostic accuracy of ChatGPT in neurological disorders***

To investigate the usefulness of informatics-aided solutions in another field, the diagnostic efficacy of a general large language model, ChatGPT, was evaluated. When provided with a short case history of neurology-related scenarios, ChatGPT was asked to deduce the 5 most likely diagnoses for each case. In parallel, medical doctors (MDs), and neurologist experts were also given the same fictional cases (Figure 12). The most likely diagnosis provided by ChatGPT matched the true diagnosis in 68.5% ± 3.28% of the cases, which significantly surpassed the success ratio of the MDs group (57.15% ± 2.64%) but did not reach the ratio of the expert group (81.66% ± 2.02%).

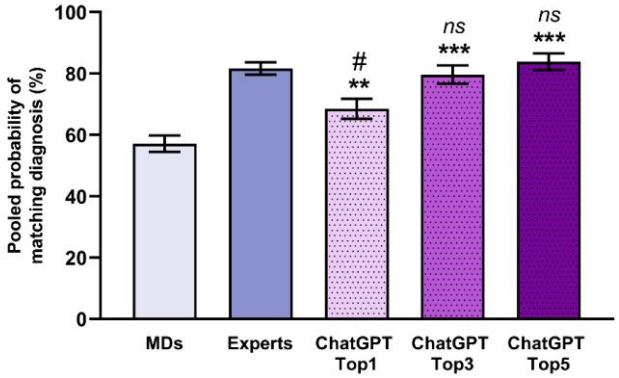


***Figure 12.*** *Diagnostic accuracy of ChatGPT in various cases, where patients presented with neurological symptoms. In the case of the ChatGPT group, three columns represent the most probable (ChatGPT Top1), three most probable (ChatGPT Top3), and five most probable diagnoses (ChatGPT Top5).*

Neurological cases were further sorted into subcategories of "acute" (n=85) and "non-acute" (n=115) cases (Figure 13). In the "acute cases" category, the most likely diagnosis provided by the AI matched 71.76% ± 4.88% of the original diagnoses, which is nearly indistinguishable from the success ratio of the MDs (Figure 13A). The "non-acute cases" subgroup represented a mixture of cases, including chronic neurological disorders, where the diagnostic procedure is often lengthy and complex, such as in the case of ALS. The diagnostic accuracy in the non-acute disease group was lower in all three groups (MDs, experts, and ChatGPT) compared to the acute neurological cases. ChatGPT achieved a diagnostic accuracy of 66.09% ± 4.41%, which was similar to the experts' diagnostic accuracy (Figure 13B).

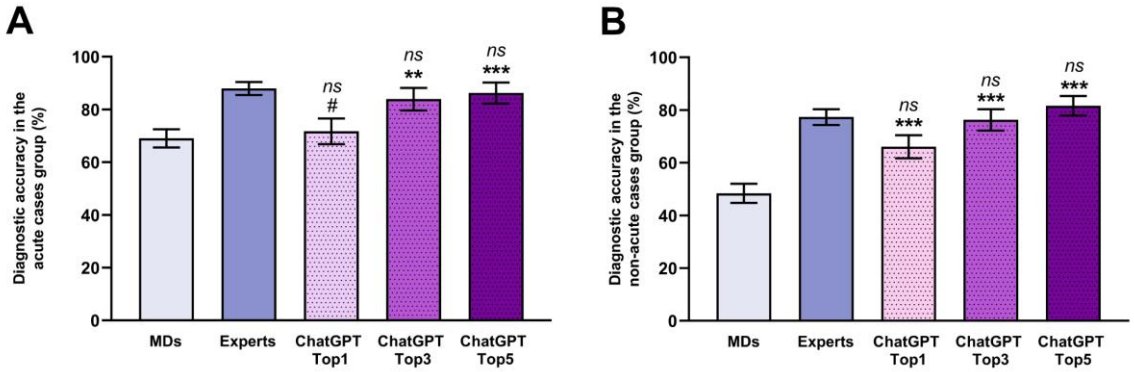


***Figure 13.*** *Pooled success ratio of correct diagnosis for (A) acute and (B) non-acute cases by medical doctors (MDs, n = 6), neurological experts (n = 6), and ChatGPT.*

**Summary**

I.

It has been demonstrated that passive transfer of blood sera from ALS patients with identified mutations resulted in elevated motoneuronal calcium level and loss of motor neurons in the spinal cord of mice

II.

It has been characterized how photobleaching alters the morphometric analysis of fluorescently labeled neurons and microglial cells, and a solution has been proposed for how this effect could be compensated

III.

It has been demonstrated that general artificial intelligence could be a valuable and precise tool in the automatization of repetitive image processing steps, and in the diagnosis of neurological diseases

## Publications providing the basis of the thesis

I. Nógrádi, B.*, **Polgár, T.F.***, Meszlényi, V., Kádár, Z., Hertelendy, P., Csáti, A., Szpisjak, L., Halmi, D., Erdélyi-Furka, B., Tóth, M., Molnár, F., Tóth, D., Bősze, Z., Boda, K., Klivényi, P., Siklós L., Patai R.. ChatGPT MD: is there any room for generative AI in neurology? *Plos One*, 19: e0310028, **2024** (IF (2024): 2.6, Journal Ranking: Q1)
*Equal contributors.

II. **Polgár, T.F**, Meszlényi, V., Nógrádi B., Körmöczy, L., Spisák, K., Tripolszki K., Széll, M., Obál I., Engelhardt, J.I., Siklós, L., Patai R.. Passive transfer of blood sera from ALS patients with identified mutations results in elevated motoneuronal calcium level and loss of motor neurons in the spinal cord of mice. *International Journal of Molecular Sciences*, 22: 9994, **2021** (IF (2021): 4.556, Journal Ranking: D1)

III. **Polgár, T.F.**, Spisák, K., Kádár, Z., Alodah, N., Szebeni, G.J., Klein, K., Patai, R., Siklós, L., Nógrádi, B. Photobleaching alters the morphometric analysis of fluorescently labeled neurons and microglial cells. *Pathology & Oncology Research*, 31: 1612087, **2025** (IF (2025): 2.3, Journal Ranking: Q2)

## Manuscripts in preparation

I. **Polgár, T.F.**, Nógrádi, B., Kádár, Z., Siklós L., Klivényi, P. Artificial intelligence-aided assessment of inflammatory alterations in murine models of amyotrophic lateral sclerosis. *In preparation.*

## Publications not included in the thesis

I. Dobra, G., Gyukity-Sebestyén, E., Bukva, M., Böröczky, T., Nyiraty, S., Bordacs, B., Várkonyi, T., Kocsis, A., Szabó, Z., Kecskeméti, G., **Polgár, T. F.**, Széll, M., & Búzás, K. Proteomic profiling of serum small extracellular vesicles predicts post-COVID syndrome development. *Clinical immunology*, 278: 110532, **2025** (IF: 4.5, Journal Ranking: Q2)

II. Ashfaq, R., Tóth, N., Kovács, A., Berkó, S., Katona, G., Ambrus, R., **Polgár, T. F.**, Szécsényi, M., Burián, K., & Budai-Szűcs, M. Hydrogel-Nanolipid Formulations for

the Complex Anti-Inflammatory and Antimicrobial Therapy of Periodontitis. *Pharmaceutics*, 17(5): 620, **2025** (IF: 5.5, Journal Ranking: D1)

III. Shaikh, K. M., Walker, C. E., Tóth, D., Kuntam, S., **Polgár, T. F.**, Petrova, N. Z., Garland, H., Mackinder, L. C. M., Tóth, S. Z., & Spetea, C.:. The thylakoid- and pyrenoid-localized phosphate transporter PHT4-9 is essential for photosynthesis in Chlamydomonas. *Plant Physiology*, kiaf158, **2025** (IF: 6.5, Journal Ranking: D1)

IV. Mészáros, M., Phan, T.H.M., Vigh, J.P., Porkoláb, G., Kocsis, A., Szecskó, A., Páli, K. E., Cser, N. M., **Polgár, T.F.**, Kecskeméti, G., Walter, R.F., Schwamborn, C. J., Janáky, T., Jan, J., Veszelka, Sz. and Deli, M. A.: Alanine and glutathione targeting of dopamine- or ibuprofen-coupled polypeptide nanocarriers increases both crossing and protective effects on a blood–brain barrier model. *Fluids Barriers CNS*, 22: 18, **2025** (IF: 5.9, Journal Ranking:)

V. Szögi, T., Borsos, B. N., Masic, D., Radics, B., Bella, Z., Bánfi, A., Ördög, N., Zsiros, C., Kiricsi, Á., Pankotai-Bodó, G., Kovács, Á., Paróczai, D., Botkáné, A. L., Kajtár, B., Sükösd, F., Lehoczki, A., **Polgár, T.F.**, Letoha, A., Pankotai, T., & Tiszlavicz, L. Novel biomarkers of mitochondrial dysfunction in Long COVID patients. *GeroScience*, 47(2): 2245-2261, **2024** (IF: 5.3, Journal Ranking: D1)

VI. Koncz, M., Stirling, T., Hadj Mehdi, H., Méhi, O., Eszenyi, B., Asbóth, A., Apjok, G., Tóth, Á., Orosz, L., Vásárhelyi, B. M., Ari, E., Daruka, L., **Polgár, T. F.**, Schneider, G., Zalokh, S. A., Számel, M., Fekete, G., Bohár, B., Nagy Varga, K., Visnyovszki, Á., … Kintses, B.: Genomic surveillance as a scalable framework for precision phage therapy against antibiotic-resistant pathogens. *Cell*, 187(21): 5901-5918, **2024** (IF: 45.5, Journal Ranking: D1)

VII. Farkas, D., Szikora, S., Jijumon, A. S., **Polgár, T. F.**, Patai, R., Tóth, M. Á., Bugyi, B., Gajdos, T., Bíró, P., Novák, T., Erdélyi, M., & Mihály, J.: Peripheral thickening of the sarcomeres and pointed end elongation of the thin filaments are both promoted by SALS and its formin interaction partners. *PLoS genetics*, 20(1): e1011117, **2024** (IF: 4.5, Journal Ranking: D1)

VIII. Devadasu E., Kanna S.D., Neelam S., Yadav R.M., Nama S., Akhtar P., **Polgár T.F.**, Ughy B., Garab G., Lambrev P.H., Subramanyam R.: Long- and short-term acclimation of the photosynthetic apparatus to salinity in Chlamydomonas reinhardtii. The role of Stt7 protein kinase. *Frontiers in Plant Science*, 14: 051711, **2023** (IF: 6.627, Journal Ranking: Q1)

IX. Mészáros M., Phan T.H.M., Vigh J.P., Porkoláb G., Kocsis A., Páli E.K., **Polgár T.F.**, Walter F.R., Bolognin S., Schwamborn J.C., Jan J.S., Deli M.A., Veszelka S.: Targeting Human Endothelial Cells with Glutathione and Alanine Increases the Crossing of a Polypeptide Nanocarrier through a Blood-Brain Barrier Model and Entry to Human Brain Organoids. *Cells*, 12(3): 503, **2023** (IF: 7.666, Journal Ranking: Q1)

X. Hudák A., Morgan G., Bacovsky J., Patai R., **Polgár T.F.**, Letoha A., Pettko-Szandtner A., Vizler C., Szilák L., Letoha T.: Biodistribution and Cellular Internalization of Inactivated SARS-CoV-2 in Wild-Type Mice. *International Journal of Molecular Sciences*, 23(14): 7609, **2022** (IF: 6.208, Journal Ranking: D1)

XI. Veszelka Sz., Mészáros M., Porkoláb G., Szecskó A., Kondor N., Ferenc Gy., **Polgár T.F.**, Katona G., Kóta Z., Kelemen L., Páli T., Vigh J.P., Walter F.R., Bolognin S., Schwamborn J.C., Jan J., Deli M.A.: A Triple Combination of Targeting Ligands Increases the Penetration of Nanoparticles across a Blood-Brain Barrier Culture Model. *Pharmaceutics*, 14(1): 86, **2022** (IF: 6.321, Journal Ranking: Q1)

XII. Kartali T., Nyilasi I., Kocsubé S., Patai R., **Polgár T.F.**, Zsindely N., Nagy G., Bodai L., Lipinszki Z., Vágvölgyi Cs., Papp T.: Characterization of Four Novel dsRNA Viruses Isolated from Mucor hiemalis Strains. *Viruses*, 13(11): 2319, **2021** (IF: 5.048, Journal Ranking: Q1)

XIII. Koderi V. S., Shetty P., Deim Z., Terhes G., Urbán E., Váczi S., Patai R., Polgár T.F., Pertics B. Zs., Schneider Gy., Kovács T., Rákhely G.: Survival Comes at a Cost : A Coevolution of Phage and Its Host Leads to Phage Resistance and Antibiotic Sensitivity of Pseudomonas aeruginosa Multidrug Resistant Strains. *Frontiers in Microbiology*, 12: 783722, **2021** (IF: 5.640, Journal Ranking: Q1)

XIV. Topal G. R., Mészáros M., Porkoláb G., Szecskó A., **Polgár T.F.**, Siklós L., Deli M. A., Veszelka Sz., Bozkir A.: ApoE-Targeting Increases the Transfer of Solid Lipid Nanoparticles with Donepezil Cargo across a Culture Model of the Blood–Brain Barrier. *Pharmaceutics*, 13(1): 38, **2020** (IF: 6.321, Journal Ranking: Q1)

XV. Papp A., Horváth T., Igaz N., Gopisetty M.K., Kiricsi M., Berkesi D.S., Kozma G., Kónya Z., Wilhelm I., Patai R., **Polgár T.F.**, Bellák T., Tiszlavicz L., Razga Z., Vezér T.: Presence of Titanium and Toxic Effects Observed in Rat Lungs, Kidneys, and Central Nervous System in vivo and in Cultured Astrocytes in vitro on Exposure by Titanium Dioxide Nanorods. *International Journal of Nanomedicine*, 15: 9939-9960, **2020** (IF: 5.93, Journal Ranking: D1)

XVI. Meszlényi V., Patai R., **Polgár T.F.**, Nógrádi B., Körmöczy L., Kristóf R., Spisák K., Tripolszki K., Széll M., Obál I., Engelhardt J.I., Siklós L.: Passive Transfer of Sera from ALS Patients with Identified Mutations Evokes an Increased Synaptic Vesicle Number and Elevation of Calcium Levels in Motor Axon Terminals, Similar to Sera from Sporadic Patients. *International Journal of Molecular Sciences,* 21(15): 5566, **2020** (IF: 5.294, Journal Ranking: D1)

XVII. Nógrádi B., Meszlényi V., Patai R., **Polgár T.F.**, Spisák K., Kristóf R., Siklós L.: Diazoxide blocks or reduces microgliosis when applied prior or subsequent to motor neuron injury in mice. *Brain Research*, 1741: 146875, **2020** (IF: 3.252, Journal Ranking: Q2)

XVIII. Zsiros O., Nagy G., Patai R., Solymosi K., Gasser U., **Polgár T.F.**, Garab G., Kovács L., Hörcsik Z.T.: Similarities and Differences in the Effects of Toxic Concentrations of Cadmium and Chromium on the Structure and Functions of Thylakoid Membranes in Chlorella variabilis. *Frontiers in Plant Science,* 11: 1006, **2020** (IF: 5.753, Journal Ranking: D1)

XIX. Kartali T., Nyilasi I., Szabó B., Kocsubé S., Patai R., **Polgár T.F.**, Nagy G., Vágvölgyi Cs., Papp T.: Detection and molecular characterization of novel dsRNA viruses related to the Totiviridae family in Umbelopsis ramanniana. *Frontiers in Cellular and Infection Microbiology*, 9: 249, **2019** (IF: 5.293, Journal Ranking: D1)

## Acknowledgements

Foremost I would like to express my gratitude to my mentor and supervisors, Dr. László Siklós (Neuronal Plasticity Research Group, HUN-REN Biological Research Centre), Dr. Bernát Nógrádi (Department of Neurology, Albert Szent-Györgyi Health Centre, University of Szeged) and Dr. Roland Patai (Neuronal Plasticity Research Group) for the support and guidance through my doctoral work.

I am grateful for all the support and work of the former members of the Neuronal Plasticity Research Group, especially Dr. Árpád Párducz, Erika Bánfiné Rácz, Zalán Kádár and Dr. Valéria Meszlényi. Without their professional help, teamwork and the inspiring and friendly atmosphere they created, this dissertation would not have been possible to write.

I would like to thank the kind support and understanding of Dr. Péter Klivényi (Department of Neurology, Albert Szent-Györgyi Health Centre, University of Szeged) and Dr. Gábor Szebeni (Laboratory of Functional Genomics, HUN-REN Biological Research Centre).

I am grateful for all the members of the Department of Biophysics and Core Facilities of the HUN-REN Biological Research Centre, and the members of the Neuroscience Research Group, University of Szeged for their support, patience and understanding.

This work was financially supported by New National Excellence Program of the Ministry for Innovation and Technology of Hungary (ÚNKP-23-3 -SZTE-315), the Gedeon Richter (PhD Excellence Scholarship 2022-2024 and Short-term Research Grant 2023), and the University of Szeged (EFOP 3.6.3-VEKOP-16-2017-00009 2020 and 2021, EKÖP-24-4 - SZTE-393 2024).